Memory effects in nematics with quenched disorder

M. Buscaglia,[1] T. Bellini,[1] C. Chiccoli,[2] F. Mantegazza,[3] P. Pasini,[2] M. Rotunno,[1] and C. Zannoni[4]
[1]*Dipartimento di Chimica, Biochimica e Biotecnologie per la Medicina, Università di Milano, Via F.lli Cervi 93, 20090 Segrate (MI), Italy*
[2]*INFN, Sezione di Bologna, Via Irnerio 46, 40126 Bologna, Italy*
[3]*DIMESAB, Università di Milano-Bicocca, Via Cadore 48, 20052 Monza (MI), Italy*
[4]*Dipartimento di Chimica Fisica ed Inorganica and INSTM, Università di Bologna, Viale Risorgimento 4, 40136 Bologna, Italy*
(Received 17 November 2005; published 17 July 2006)

We present a combined experimental and Monte Carlo study of a nematic phase in the presence of quenched disorder. The turbidity of a nematic liquid crystal embedded in a porous polymer membrane is measured under different applied field conditions for field-cooled and zero-field-cooled samples. We find that a significant permanent alignment of the nematic can be induced by fields as low as 0.1 $V/\mu m$ applied during the isotropic to nematic transition. An analogous effect and dependence on sample history is found by studying the order parameter of a sprinkled disorder Lebwohl-Lasher spin model, indicating that dilute quenched randomness is sufficient to produce memory effects in nematics. The large memory induced by field cooling appears to be written in the system during the transition as a result of the field action on freely oriented nematic nuclei. At lower temperature the nuclei consolidate into permanent nematic textures developed from the interaction with quenched disorder.

DOI: 10.1103/PhysRevE.74.011706 PACS number(s): 61.30.Jf, 61.30.Cz, 61.30.Gd, 61.30.Pq

I. INTRODUCTION

Nematics with quenched disorder represent technologically relevant soft materials showing a variety of novel properties accessible to experimental investigations [1–3]. Nematic liquid crystals (NLC) embedded in disordering host structures are typically very opaque and thus characterized by large optical turbidity, τ. This is a consequence of the birefringence of liquid crystals (LC) and of the spatial fluctuations of the optical axis induced by disorder [4,5]. The application of an electric field (E) forces alignment and hence decreases fluctuations, in turn reducing τ [1]. Generally, after the removal of the field, nematics in cells with a simple geometry recover the unperturbed state defined by boundary conditions and elasticity. A peculiar feature of nematics in complex geometries is instead their memory of applied fields, consisting of a permanent change of τ after the removal of the field. Several examples of nematics mixed with dispersions of particles or macromolecules have been reported to have a memory of applied fields [6]. However, the origin of multistability in these systems is typically ascribed to dynamic restructuring of the dispersions rather than to the topology of the nematics. Phenomena of multiple stability of the ordering of LC have been found in systems with specifically designed and highly controlled surface geometry [7] and surface anchoring [8], indicating that pure nematics can actually be trapped in various topological states by means of carefully designed boundary conditions. Memory effects have also been observed in nematics disordered by "quenched" hosting structures where the NLC is forced to have random orientations of the director and chaotically entangled defects. It has been shown that the orientational order of NLC embedded in a fractal network of silica gel jams into a kind of glassy state [9]. Long term memory and history dependence have been found by studying nematics incorporated in other randomly interconnected polymeric structures [10,11].

Because of the orientational character of their ordering, nematics have often been compared with magnets despite obvious differences in their nature, symmetry, and phase behavior. The polar magnetic ordering develops along the ferromagnetic axis through a second order transition, while the appearance of the nonpolar nematic ordering breaks the continuous angular symmetry in a discontinuous transition. In particular, since the first investigations of nematics in random environment in the 1990s, it has been tempting to draw analogies with the behavior of magnets in random field that were widely studied and debated in the 1980s [12]. Conceptual tools were borrowed, such as the Imry-Ma argument, whose correctness was finally established for random magnets. The argument predictions are that the 3D Ising magnet survives the presence of a random field, while continuous symmetry systems, such as nematics, should lose their long range ordering under any applied random field strength. Experiments on both systems [12,13] indicate this is actually the case. Even more intriguing is the fact that random magnets, analogous to disordered nematics, show multistability and history dependence, such that the ground state order is attained when samples are zero field cooled, while field cooling treatment leads to systems "trapped" in a metastable disorder [12]. The long term stability of the disordered state is due to the pinning of domain walls by lattice vacancies [12]. Indeed, an analogous role of defect pinning was proposed in a recent investigation. The origin of memory effects in disordered nematics was examined by means of Monte Carlo (MC) simulations on a random-field Lebwohl-Lasher spin model, specifically the sprinkled silica spin (SSS) model [14]. We found that the disordered nematic structure can be ascribed to the spatial distribution of pinned defect lines and that memory stems from the pinning of these strings [15].

Here we present a study based on experiments and MC simulations examining the effects of an external electric field on nematics with quenched disorder. We show that the topological structure of the nematics strongly depends on the

combined temperature and applied field histories. We characterize the response of the experimental system to the applied field, and we monitor the memory after the removal of the field. We show that a field applied while cooling through the isotropic (I) to nematic (N) transition induces a much more pronounced alignment than a similar field applied in the nematic phase. We also performed extensive MC simulations on a SSS model mimicking the experimental sequences of temperature changes and applied field. The observed analogies between experimental and simulated behaviors confirm the simple SSS model as a valid tool for the study of the mechanism of memory in nematics with quenched disorder. Specifically, the success of MC modeling demonstrates that quenched disorder by itself is sufficient to account for memory effects.

II. EXPERIMENT

The experimental investigation was carried out on a system of mixed cellulose ester (MCE) membranes (MF millipore membrane filters) soaked with 4-cyano-4′-*n*-pentyl-biphenyl (5CB) liquid crystal. The membranes have a mean pore size of 3 μm with 17% of the total volume fraction occupied by the solid material having a refractive index of $n_{MCE}=1.51$. In order to obtain thin membrane slices, the commercially available filter discs were embedded in paraffin wax, sliced by means of a microtome, and thoroughly washed with xylene to remove the wax. The sliced membranes were dried, spread with 5CB, and heated above the N to I transition temperature ($T_{NI}=32.5$ °C) in a vacuum oven for three hours to eliminate the residual air. The samples used in the experiments were sandwiched between indium tin oxide (ITO) coated glass slides resulting in a membrane thickness of about 16 μm, measured by means of micrometer and optical microscopy. In order to prevent dielectric breakdown, the ITO coatings of the cell were previously patterned to avoid an air gap through the electrodes. The residual coating was removed by selectively etching with hydrochloric acid. The applied voltage had a sinusoidal wave form with 1 kHz frequency and amplitudes from 0 V to 180 V. The samples were held in a thermally controlled oven. We measured the intensity of a 4 mm diameter He -Ne laser beam transmitted through the samples in the direction of the applied field. Transmitted light was selected by spatially filtering the beam before and after the sample. The sample turbidity was calculated as $\tau=-\ln(I_T/I_0)/d$, where I_T/I_0 represents the transmitted light (I_T) referred to the incident (I_0), and d is the thickness of the sample cell. We produced several cells containing MCE+5CB samples and for all samples we measured a value of turbidity at 25 °C of $0.37(\pm 0.01)$ μm^{-1}. In order to allow an easy comparison between different sets of data, we present results obtained from one representative sample.

The disordered nematic samples were prepared by two different methods: in the zero-field-cooling (ZFC) procedure (Fig. 1) the sample was cooled down from the isotropic phase with no field applied. In the field-cooling (FC) procedure (Fig. 2), an electric field was applied to the sample in the isotropic phase at 36 °C and kept on while the temperature was decreased to 25 °C, when the field was then turned off.

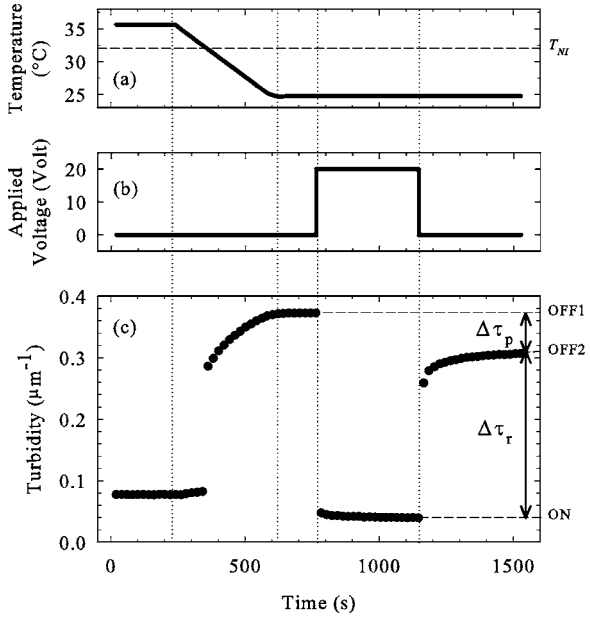

FIG. 1. Experimental ZFC procedure and response to the electric field. (a) The temperature was decreased linearly from the I phase to the N phase, and then held constant. (b) The electric field applied to the sample was turned on after the equilibration in the N phase and removed after 6 min. (c) The turbidity of the sample increases as the temperature decreases in the N phase. The application of an electric field in the N phase induces a pronounced decrease of the turbidity which is partially ($\Delta\tau_r$) recovered after the removal of the field. The unrecovered part ($\Delta\tau_p$) is ascribed to permanent reconfiguration of the system. The vertical dotted lines are drawn as a guide to the eye in correspondence of temperature gradient changes and field transitions.

The turbidity of the sample in the I phase is independent of the applied field strength and is ascribed to the mismatch of the refractive index between the isotropic LC and the MCE matrix. The sample prepared by the ZFC procedure (Fig. 1) showed a high turbidity ($\tau=0.375$ μm^{-1}) in the N phase in the absence of an applied field, since the disordering MCE structure induces pronounced orientational fluctuations of the optical axis of the nematic.

The detailed behavior of the turbidity as a function of temperature has been shown to depend on the average size of the nematic domains [5]. Upon the application of an external electric field, the turbidity of the system rapidly decreases with a relaxation time of a few milliseconds [16] affecting about 90% of the total turbidity change. Only the remaining 10% of the turbidity is characterized by a much slower settling time. The field was removed after 6 min, when the system was fully equilibrated. In this case too, the system undergoes a fast relaxation and a slower recovery with smaller amplitude. Repeated application of similar field pulses with the same amplitude did not show any significant dependence of the turbidity on the number of pulses. The turbidity at equilibrium, after the removal of the field, was lower than the turbidity measured in the N phase before the application of the field. The difference between those values, $\Delta\tau_p$, rep-

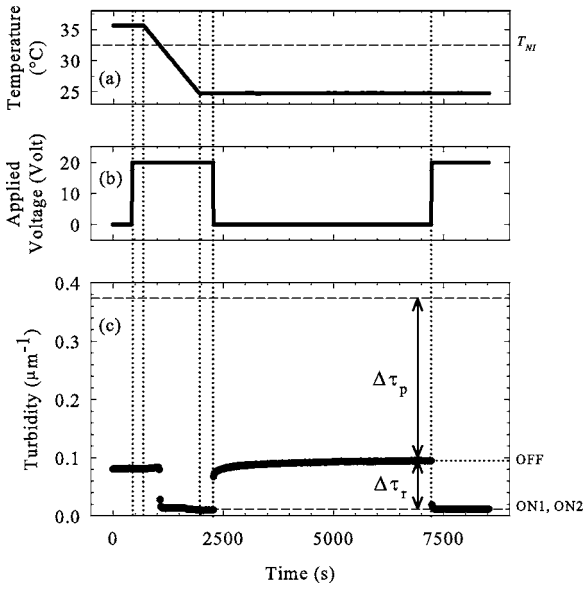

FIG. 2. Experimental FC procedure and response to the electric field. (a) Similar to the ZFC procedure, the temperature of the sample was decreased linearly to bring the sample from the *I* phase to the *N* phase, and then held constant. (b) The electric field applied to the sample was turned on in the *I* phase and maintained until the sample was equilibrated in the *N* phase. The field was kept off for 5000 sec and then turned on again. (c) The turbidity of the sample in the *I* phase is not influenced by the application of the electric field. In the *N* phase the sample turbidity is low because of the aligning effect of the applied field. Upon removal of the field the high turbidity measured in the unperturbed ZFC state (dashed horizontal line at τ=0.375 μm^{-1}) is partially recovered ($\Delta\tau_r$). The unrecovered part ($\Delta\tau_p$) is ascribed to permanent reconfiguration induced by the field. The subsequent application of an electric field induces a pronounced decrease of the turbidity. The vertical dotted lines are drawn as a guide to the eye for temperature gradient changes and field transitions.

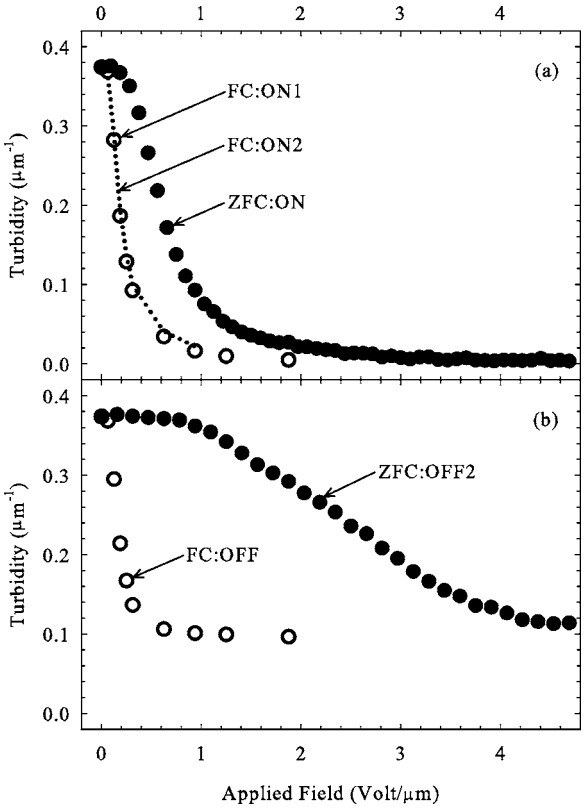

FIG. 3. Turbidity measured at 25 °C as a function of the amplitude of an external electric field *E*. (a) Turbidity measured in presence of the applied field. Full dots: ZFC:ON states. These data have been taken by applying consecutive bursts of the electric field having increasing amplitude. The burst duration is 6 min, with a time interval of 6 min between two consecutive bursts. Open dots: FC:ON1 states. Dotted line: FC:ON2 states. Each point refers to an independent FC measure following the field *E* and temperature state sequence ON1-OFF-ON2 as shown in Fig. 2. (b) Turbidity measured after the removal of the electric field. Full dots: ZFC:OFF2 states. These data have been taken after the application of consecutive burst of duration 6 min. Each value of turbidity has been measured 6 min after the removal of the field. Open dots: FC:OFF states. Each point refers to an independent FC measure following the field and temperature state sequence ON1-OFF-ON2 as shown in Fig. 2.

resents a measure of the remnant order induced by the field and thus provides a quantitative representation of the induced memory. The residual order can be wiped out by means of a *N* to *I* phase transition, and the procedure described in Fig. 1 can be repeated indefinitely.

The same sample was used to show the effect of the FC procedure (Fig. 2). In this case an identical electric field was applied in the *I* phase, and then the temperature was decreased. Different from the ZFC case, the turbidity decreases entering the *N* phase and stabilizes to a very low value at 25 °C. Upon removal of the field, the sample undergoes a faster visco-elastic relaxation followed by a slower glassy equilibration, as also found in other disordered nematic systems [11]. The asymptotic value of the turbidity is much lower than the one measured in the unperturbed system at the same temperature, and it is also lower than the value of turbidity measured in the ZFC procedure after the removal of the field. Consequently, the remnant order $\Delta\tau_p$ induced by the field in the FC procedure is significantly higher than the one measured on the same sample prepared with the ZFC procedure. Moreover, the subsequent application of an electric field after the FC procedure induces a high level of transparency, similar to the one observed before the removal of the field in the FC preparation.

Following the experimental scheme reported in Figs. 1 and 2, two procedures were undertaken and are characterized by sequences of electric field states: OFF1-ON-OFF2 and ON1-OFF-ON2 for the ZFC and FC preparation, respectively. Since the turbidity of the sample depends on the history of applied field and temperature, each of the resulting six states is characterized by its own equilibrium turbidity. We shall refer to those field states as ZFC:OFF1, ZFC:ON, ZFC:OFF2, FC:ON1, FC:OFF, and FC:ON2.

Figure 3(a) reports the values of turbidity measured in the ON states for both preparations as a function of the applied field. The values measured in the ZFC:ON state are characterized by a pronounced decrease for field strength of approximately 1 V/μm (I_T/I_0=1/2 for 1.35 V/μm). The mea-

sured turbidity becomes negligible for field values higher than 3 $V/\mu m$. The high level of transparency at high field is a consequence of the overall alignment of the nematic and of the refractive index matching between the MCE membrane and the ordinary axis of the LC. The effect of the applied field is clearly more pronounced in the FC experiment. The field threshold for transparency ($I_T/I_0=1/2$) for either FC:ON1 or FC:ON2 is about 0.6 $V/\mu m$, and the saturation level is reached at about 1.2 $V/\mu m$. The two FC states do not differ consistently in terms of turbidity, but they are significantly different from the ZFC state, showing that the field applied during the FC procedure induces a more pronounced alignment which permanently increases the system susceptibility to applied fields.

Figure 3(b) shows the turbidity measured at equilibrium after the removal of an applied electric field. The difference, $\Delta\tau_p$, between each point and the value at 0 $V/\mu m$ represents a measure of the sample memory after the removal of the field (ZFC:OFF2 and FC:OFF). Considering the ZFC:OFF2 state, the memory induced by the applied field is negligible for field strengths lower than 1 $V/\mu m$. However, the FC:OFF state is characterized by a high level of residual transparency after the removal of fields as low as 0.1 $V/\mu m$. This can be inferred by comparing the turbidity of the FC:ON1 and FC:ON2 states [open dots in Fig. 3(a)] to the turbidity of the FC:OFF state [open dots in Fig. 3(b)]. After the removal of high fields both the ZFC and FC samples relax to a common saturation level for the remnant turbidity close to 0.1 μm^{-1}, which is significantly higher than the values measured in the ON states at high field.

III. SIMULATION MODEL

The dependence of the sample alignment on its temperature and applied field history was investigated by MC simulations performed on the SSS model proposed in Ref. [14]. This is a Lebwohl-Lasher lattice system [17], where a fraction of the spins, randomly chosen, has an orientation selected at random and kept fixed to mimic the quenched disorder [13]. The SSS model has some connection with the uniform random field Hamiltonian, where each spin is subjected to a random perturbation [18–20]. However, it has, in our opinion, some distinctive advantages for the present problem, such as the possibility of varying the concentration of impurities as well as the introduction of dopant localization.

The system is thus composed of two sets of spins $\mathbf{s_i}$: $\mathcal{N}$ free to reorient spins describing the NLC, and $\mathcal{S}$ frozen spins (FS) introducing quenched disorder in the system. The amount of disorder is expressed by the concentration of frozen spins $p=\mathcal{S}/(\mathcal{N}+\mathcal{S})$. The Hamiltonian of the system is

$$H_{SSS} = -\epsilon\left(\sum_{\langle i,j\rangle\in(\mathcal{N}\cup\mathcal{S})} P_2(\mathbf{s_i}\cdot\mathbf{s_j}) + \eta\sum_{i\in\mathcal{N}} P_2(\mathbf{s_i}\cdot\mathbf{z})\right), \quad (1)$$

where $\mathbf{s_i}$ and $\mathbf{z}$ are unit vectors representing the ith spin orientation and the direction of the applied field, respectively, P_2 is the second Legendre polynomial, and the indexes i,j run on nearest neighbors $i<j$. The second term in Eq. (1) represents the coupling to the applied field. The positive constants ϵ and η express scaling factor for the energy and the field-spin coupling, respectively. The evolution of the system has been studied, using a Monte Carlo–Metropolis algorithm [21] on cubic lattice samples of linear size $L=50$ and with $p=0.14$. The MC scheme adopted consists of standard single spin rotational moves that can be assimilated to physical reorientations of the real particles. In this sense, even though the MC dynamics are arbitrary, the chosen representation can be related to a plausibly real one. The MC cycles can be considered, to an arbitrary scaling factor, as time units. We have followed the value of the nematic order parameter $\langle P_2\rangle$ computed on the free spins. In the absence of the external field ($\eta=0$) the system order parameter is defined only by the reduced temperature $T^*=k_BT/\epsilon$.

For the value of L and p considered in this work, the I to N phase transition occurs at $T^*_{NI}=0.75(\pm0.1)$. Each simulation run starts from a randomly oriented spin configuration in the I phase at $T^*_I=1.2$. In order to mimic the ZFC and the FC experiments, the simulated system is cooled down to the N phase at $T^*_N=0.2$ using different values for the field-spin coupling parameter η. The temperature $T^*_N=0.2$, very deep in the N phase, is used to avoid effects of thermal fluctuations as already done in previous works on similar systems [11,13,21], taking advantage of the absence of smectic phases in the model.

The value of $\langle P_2\rangle$ in the equilibrated N state is not found to depend significantly on the cooling rate. We show results obtained after at least 10^5 cycles, a MC time more than sufficient to reach equilibrium for the N phase without disorder [21]. The value of $\langle P_2\rangle$ for these equilibrated states is generally overestimated because of finite-size effects and decreases with increasing lattice size [11]. Figure 4 shows the behavior of $\langle P_2\rangle$ as a function of the number of MC cycles after the temperature change $T^*_I\rightarrow T^*_N$ using two different values of the field parameter, $\eta=0$ and $\eta=0.01$. After 1×10^5 and 2×10^5 cycles the values of the external field η are reversed and the simulations stop at 3×10^5 MC cycles. In analogy to the experiments, three field states can be defined at equilibrium either for the ZFC or for the FC procedure, resulting in the same six field states introduced in the experimental section (ZFC:OFF1, ZFC:ON, ZFC:OFF2, FC:ON1, FC:OFF, FC:ON2). The order parameter of the equilibrated system after ZFC (ZFC:OFF1 state) is small but not negligible because of the finite-size effect. In fact, the $\langle P_2\rangle$ of this system approaches zero with increasing lattice size as reported in [11,13]. The application of the external field (ZFC:ON state) induces an increase in the average order parameter and after the subsequent removal of the field (ZFC:OFF2 state), the system does not recover completely to the original value of $\langle P_2\rangle$, similarly to the experimental behavior.

The analogy with the experiments is also strong in the case of the FC procedure. A certain value of the external field η applied during the I to N transition (FC:ON1) induces a higher alignment and after the removal of the field (FC:OFF), the system retains a relatively high level of alignment even after 10^5 cycles. Finally, a further application of the field (FC:ON2) induces a value of $\langle P_2\rangle$ similar to the one found in the FC:ON1 state. The value of the order parameter $\langle P_2\rangle$ in the presence of an external field of strength η is

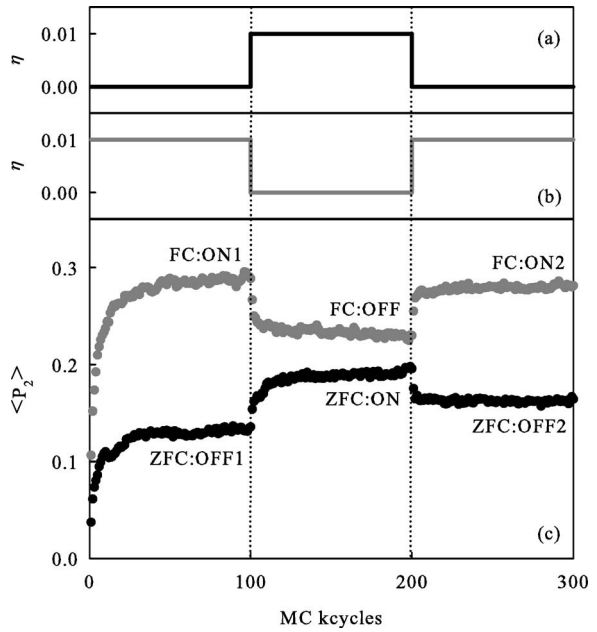

FIG. 4. A schematic example of ZFC and FC procedure adopted in the MC simulations of the SSS model as a function of the Monte Carlo (MC) kcycles. (a) In the ZFC procedure the system was brought from the I phase to the N phase with $\eta=0$, then the field was turned on at 1×10^5 cycles and removed again at 2×10^5 cycles. (b) In the FC procedure the system was equilibrated in the N phase with $\eta=0.01$, then the field was removed at 1×10^5 cycles and turned on again at 2×10^5 cycles. (c) Nematic order parameter $\langle P_2\rangle$ versus MC cycles as obtained from the simulation using the ZFC procedure (black points) and the FC procedure (gray points) with $p=0.14$ at $T_N^*=0.2$. The MC cycles are counted starting from the temperature change $T_I^*\rightarrow T_N^*$. The vertical dotted lines are drawn as a guide to the eye for the field transitions.

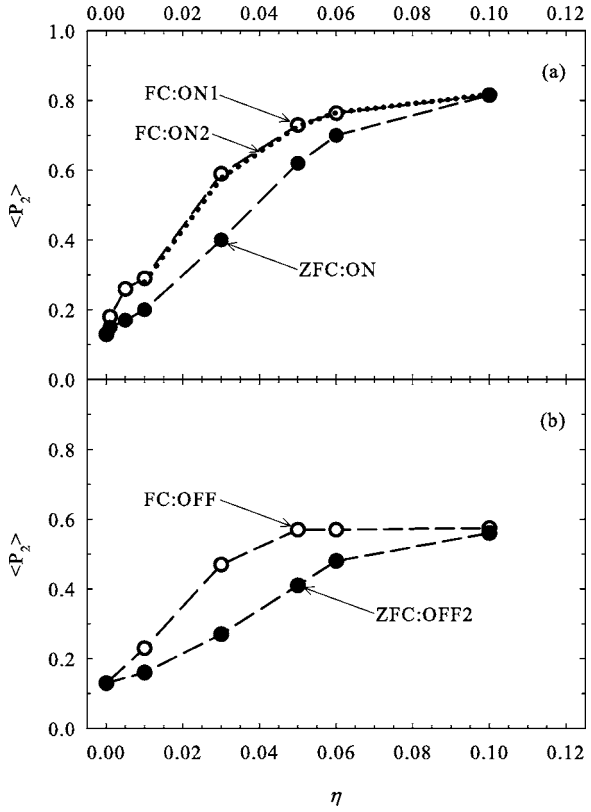

FIG. 5. Order parameter $\langle P_2\rangle$ obtained from MC simulations as a function of an external field of strength η. (a) Order parameter obtained in presence of the external field. Full dots joined by the dashed line: ZFC:ON states. These data have been obtained by applying consecutive pulses of field of increasing amplitude η and letting equilibrate after each field transition (see Fig. 4). Open dots joined by the dashed line: FC:ON1 states. Dotted line: FC:ON2 states calculated for $\eta\geq0.1$. Each points refers to an independent FC simulation, following the field state sequence ON1-OFF-ON2 as shown in Fig. 4. (b) Order parameter obtained after the removal of the external field. Full dots: ZFC:OFF2 states. These data represent the residual $\langle P_2\rangle$ computed after the removal of a field of strength η (see Fig. 4). Open dots: FC:OFF states. Each point refers to an independent FC simulation, following the field state sequence ON1-OFF-ON2 as shown in Fig. 4.

shown in Fig. 5(a). In general, $\langle P_2\rangle$ increases as the field increases. In the case of ZFC:ON state, the maximum slope of the curve $\langle P_2\rangle$ vs η is obtained for a field strength $\eta=0.03\pm0.01$. Differently, the $\langle P_2\rangle$ computed for the FC:ON1 and FC:ON2 states is characterized by a steeper slope for small values of η, thus giving higher level of ordering for low field strengths. Analogously, the residual order after the removal of the field, increases with increasing field strength η, and it is higher in the FC:OFF state than in the ZFC:OFF2 state, as shown in Fig. 5(b). In the limit of large η the order parameters $\langle P_2\rangle$ of both states reach the same plateau value.

IV. DISCUSSION

The results reported in the experimental section show that in the systems of nematics with quenched disorder investigated in this work, an external electric field may induce permanent alignment. Given a certain temperature and applied field, the value of the turbidity is not well defined. The system assumes different stable configurations characterized by different values of turbidity, depending on the thermal and applied field history. Thus, the nematics disordered by the MCE matrix shows multistability. Analogously, in the simulation model the presence of the randomly oriented frozen spins also leads to a history dependence of the order parameter $\langle P_2\rangle$. Both the turbidity measured in the experiments and the order parameter computed from the model indicate the degree of alignment of the systems. Indeed, by means of an appropriate scattering model for the experimental system, the measured turbidity can be converted into the corresponding value of the nematic order parameter. We have developed such a scattering model based on the observation that in nematics with quenched disorder the nematic correlation function is consistent with a short range nematic order [13]. Thus, the system can be envisioned as a collection of nematic domains with random orientation, and the turbidity can be calculated from the scattering cross section of suitable uniaxial spherical domains [5]. The orientational distribution of the domains is modified by the external field through a simple viscoelastic interaction, which has been shown to describe the nonlinear response of disordered nematics to ap-

plied fields [16]. In this way, the computed values of turbidity can be numerically converted in the equivalent value of the average order parameter computed on the domain orientations, $\langle P_2 \rangle_d$ [11]. Considering different choices for the physical parameters characterizing the NLC and the disordering structure, the following relationship has been found to empirically link the computed values of τ and $\langle P_2 \rangle_d$ [22]:

$$\langle P_2 \rangle_d = 1 - \frac{\tau}{\tau_0}, \tag{2}$$

where τ_0 is the value of turbidity corresponding to a uniform distribution of the domain orientation and coincides with the turbidity of the unperturbed disordered nematic. We found that the linear relationship between τ and $\langle P_2 \rangle_d$ as in Eq. (2) leads to significant errors only for very low values of τ. Equation (2) allows a direct comparison between the turbidity measured in the experiments and the order parameter computed in the simulations. Taking into account Eq. (2), the experimental behaviors shown in Fig. 3 exhibit strong analogies with the computed $\langle P_2 \rangle$ reported in Fig. 5. In particular, the alignment of the nematic domains, as given by Eq. 2, induced by FC fields lower than 0.2 V/μm or $\eta < 0.06$ is almost completely maintained after the removal of the field, as can be inferred comparing the FC:ON1 and FC:OFF turbidities in Figs. 3 and 5. Moreover, the subsequent application of a field of equal strength [FC:ON2 state in Figs. 3(a) and 5(a)], restores almost the same level of alignment induced by the initial FC field. Differently, the aligning effect of a similar field applied on a ZFC sample is significantly lower [ZFC:ON state in Figs. 3(a) and 5(a)].

In order to quantify the analogies between the experiments and simulations, we have introduced an indicator for the fraction of field induced alignment which is maintained after the removal of the field, for both the FC and ZFC procedure. For the simulated system, this memory indicator (m_{sim}) can be defined as

$$m_{sim} = \frac{\langle P_2 \rangle_{OFF} - \langle P_2 \rangle_0}{\langle P_2 \rangle_{ON} - \langle P_2 \rangle_0}, \tag{3}$$

where $\langle P_2 \rangle_0$ is the order parameter of the unperturbed disordered system (ZFC:OFF1 state), $\langle P_2 \rangle_{ON}$ is computed with $\eta > 0$, and $\langle P_2 \rangle_{OFF}$ is the residual order parameter calculated after the removal of the field. According to Eq. (2), an analogous memory coefficient can be coherently defined for the measured experimental turbidity. The order parameter of the simulated model in Eq. (3) can be replaced with the domain order parameter $\langle P_2 \rangle_d$ for the experimental system, leading to

$$m_{exp} = \frac{\Delta\tau_p}{\Delta\tau_p + \Delta\tau_r}, \tag{4}$$

where $\Delta\tau_p$ and $\Delta\tau_r$ are shown in Figs. 1 and 2. Both measured and simulated memory coefficients are equal to zero when the system recovers completely after the removal of the applied field and are instead close to one when it maintains the induced alignment. Figure 6 shows the values of m_{exp} computed for the data reported in Fig. 3 and the values of m_{sim} for the data of Fig. 5. Comparison of experimental and simulated memory coefficients reveals some basic similarities. The fractional permanent alignment monotonically increases if the field is applied after the ZFC sample preparation, and decreases after a low field maximum, if the field is applied during the FC procedure. Additionally, both preparations lead to an asymptotic value of the memory coefficient of about 0.64 for the simulations and 0.72 for the experiments. These surprisingly good results confirm that the simple SSS model captures at least the basic features of these complex systems with sufficient accuracy to yield the same memory effects found in nematics with quenched disorder. However, the high value of the ZFC m_{sim} extrapolated to $\eta = 0$ ($m_{sim} \approx 0.5$), compared to the negligible value of the corresponding m_{exp}, indicates a difference between experiments and simulations. The simulated system seems permanently slightly deformed by arbitrarily small fields, yielding an apparent threshold-free mechanism for the corresponding memory.

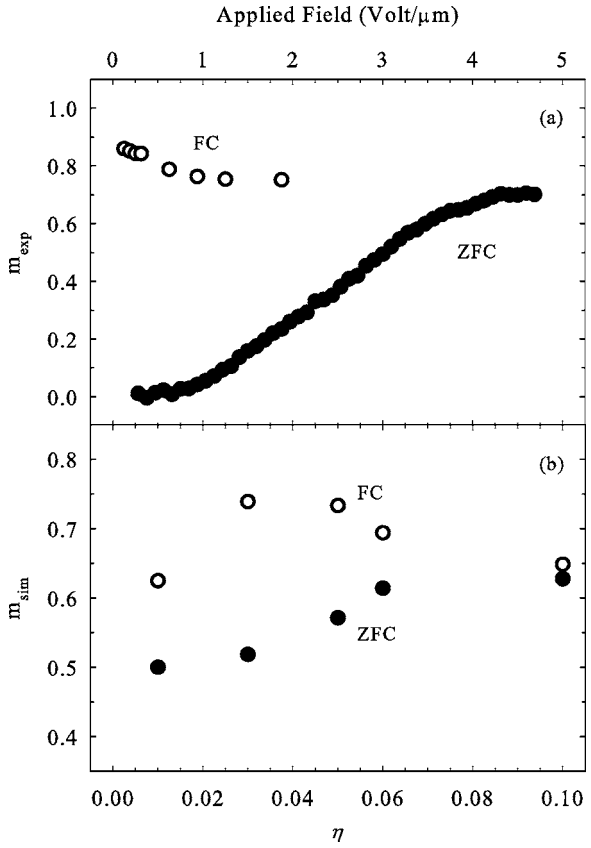

FIG. 6. Experimental (m_{exp}) and simulated (m_{sim}) memory coefficient as a function of the external field. (a) m_{exp} measured for fields applied during ZFC (full dots) and FC (open dots) procedures. Points at very low fields (below 0.25 V/μm for ZFC and below 0.1 V/μm for FC) are not shown since the low values of $\Delta\tau_p$ and $\Delta\tau_r$ lead to high experimental uncertainty in the extraction of m_{exp}. (b) m_{sim} calculated for fields η applied during ZFC (full dots) and FC (open dots) procedures.

The actual role played by the specific properties of the MCE surface and structure on the origin of memory in the experimental system is still the object of study by several groups. Other kinds of disordering structures have been

found to induce multistability of the nematic ordering under specific conditions. Dispersions of either hydrophilic or hydrophobic silica nanoparticles in a few percent of volume fraction have also been reported to show permanent alignment induced by an electric field [23,24]. However, in those systems, the robustness of the disordering silica structure can be argued against and consequently local reordering of the silica matrix under the effect of the field cannot be completely ruled out. For example, repeated cycling through the *I-N* transition in the presence of large magnetic fields has been reported to produce anisotropic disordering matrices [25]. On the other hand, the more bulky arrangement of the MCE matrix studied in the present work can hardly allow a structural change under the weak electric forces employed here. The origin of the memory might be ascribed to the change of anchoring of the nematics on the MCE surface under the effect of the field. However, the reported time scale for the phenomena involving surface anchoring changes mediated by external fields [8] is typically longer than the duration of the applied fields employed in this work. Moreover, the surface LC alignment induced by field cooling procedures on relatively strong anchoring substrates is reported to be stable against *N-I-N* thermal cycles [8]. However, for both the ZFC and FC experimental procedure, our MCE+NLC samples are found to return to their spontaneous high turbidity states after an arbitrarily short thermal cycle to the *I* phase. This observation suggests that the presence of memory does not imply multistability of the anchoring conditions. The fact that memory is found in the simulations, where neither spatial nor orientational rearrangement of frozen spins is allowed, indicates that the origin of memory is an effect of the frustration in the topology of random field nematics. Additionally, we find that the energies computed for all the equilibrated states at zero field [shown in Fig. 5(b)] differ from each other by less than 0.2%, which is comparable to the computational uncertainty given by the amplitude of the equilibrium fluctuations of the order parameter. When combined, these elements support the idea of a system (both experimental and simulated) composed of an ensemble of interacting nematic domains characterized by a multitude of available topological states having similar free energies but different orientational configurations. These degenerate orientational configurations are likely to be separated by energy barriers whose heights are significantly larger than k_BT, since even increasing the observation time from hours to weeks the remnant order does not appear to relax [11].

The particular orientational distribution of the nematic domains is somehow recorded in the system during the *I* to *N* transition. This may be rationalized assuming that in the *N* phase for temperature below close enough to T_{NI} the system is in the coexistence region: nematic nuclei are surrounded by isotropic liquid and thus they should be rather insensitive to each other and to the disordering matrix. The existence of an extended temperature range of coexistence has been recently reported for systems of NLC disordered by dispersions of hydrophilic silica nanoparticles [4]. When the electric field is applied in such a temperature range, the nematic nuclei orient parallel to the field with virtually no constraints. As the temperature is decreased, the nematic fraction grows and the ordered clusters interact with each other and with the disordering matrix. The specific continuous texture connecting domains and solid interfaces determines the topology "written" in the sample by the cooling procedure. The temperature at which such topological texture is set has been described as the conversion from a random dilution to a random field regime and is marked, in the aerosil-disordered LC, with a second specific heat peak at temperature below T_{NI} [4]. According to this description, this behavior is a peculiarity of first order phase transitions in the presence of quenched disorder, suggesting that in the comparison between disordered nematics and other seemingly analogous systems, like random magnets, the discontinuous character of the *NI* transition must be taken into account.

The existence of a temperature range below T_{NI} in which free nematic domains coexist with the isotropic phase, is manifested by the remarkable difference in the FC vs ZFC memory coefficients m_{exp} and m_{sim} in Fig. 6, indicating that at low fields the ZFC response is fully elastic while the FC response is predominantly plastic with no apparent strain threshold. Apparently, the largest nematic nuclei, i.e., those most susceptible to respond to small fields and providing large FC m_{exp}, are also the least constrained by the disordering structure at the onset of the random field regime. The key role of the nematic texture connecting domains to each other and to the disordering structure has been analyzed in terms of the topology of defect lines [15]. It has been found that the different equilibrated states in systems evolving from different initial conditions can be entirely ascribed to different populations of the long defect lines surrounding the nematic domains.

V. CONCLUSIONS

We have shown that an external electric field may induce permanent alignment in nematic LC embedded in a disordering MCE structure. The turbidity of the sample strongly depends on the history of temperature and applied field. An external field applied during the *I* to *N* phase transition typically has a much stronger aligning power than the same field applied to the sample in the unperturbed *N* state. By means of the FC procedure, the sample is permanently aligned using a field strength lower than 0.1 $V/\mu m$. The resulting system can be repeatedly switched between a transparent and an opaque state with field strengths much lower than the one needed to orient the unperturbed nematic. We have shown that memory effects is induced by an external field applied to the simple SSS model, in good agreement with the experimental results. The behavior of the computed order parameter versus the field strength qualitatively resembles the estimated nematic order parameter of the experimental system, showing the same difference between ZFC and FC. These results confirm that the simple SSS model embodies sufficient ingredients to account for the mechanism behind the memory in nematics with quenched disorder. We interpret the large FC memory to be due to the alignment of nematic domains in the coexistence region, consolidated by the nematic texture developed at lower temperatures. Such a texture

encloses topological defect lines whose paths are specific for each given state. Accordingly, the multitude of stable configurations in nematics with quenched disorder may arise from the variety of topological configurations stabilized by the pinning of the defect lines to the disordering structure.

ACKNOWLEDGMENTS

We acknowledge support by INFN Grant No. I.S. BO12 (C.C. and P.P.); MIUR (Grant No. COFIN 2005035119), and University of Bologna (C.Z.); MIUR (Grant No. COFIN 2004024508) (T.B.); and CNR-INFM (T.B., M.B., and F.M.).

[1] *Liquid Crystals in Complex Geometries Formed by Polymer and Porous Networks*, edited by G. P. Crawford and S. Zumer (Taylor and Francis, London, 1996).
[2] T. Bellini, N. A. Clark, C. D. Muzny, L. Wu, C. W. Garland, D. W. Schaefer, and B. J. Oliver, Phys. Rev. Lett. **69**, 788 (1992).
[3] G. S. Iannacchione, S. Qian, D. Finotello, and F. M. Aliev, Phys. Rev. E **56**, 554 (1997).
[4] M. Caggioni, A. Roshi, S. Barjami, F. Mantegazza, G. S. Iannacchione, and T. Bellini, Phys. Rev. Lett. **93**, 127801 (2004).
[5] T. Bellini, N. A. Clark, V. Degiorgio, F. Mantegazza, and G. Natale, Phys. Rev. E **57**, 2996 (1998).
[6] M. Kreuzer and R. Eidenschink, *Liquid Crystals in Complex Geometries Formed by Polymer and Porous Networks* in (Ref. [1]), Chap. 15.
[7] E. L. Wood, G. P. Bryan-Brown, P. Brett, A. Graham, J. C. Jones, and J. R. Hughes, SID Symposium Digest **31**, 124 (2000).
[8] S. Faetti, M. Nobili, and I. Raggi, Eur. Phys. J. B **11**, 445 (1999).
[9] X-l. Wu, W. I. Goldburg, M. X. Liu, and J. Z. Xue, Phys. Rev. Lett. **69**, 470 (1992).
[10] R. Yamaguchi and S. Sato, Liq. Cryst. **14**, 929 (1993).
[11] T. Bellini, M. Buscaglia, C. Chiccoli, F. Mantegazza, P. Pasini, and C. Zannoni, Phys. Rev. Lett. **88**, 245506 (2002).
[12] D. P. Belanger and A. P. Young, J. Magn. Magn. Mater. **100**, 272 (1991), and references therein.
[13] T. Bellini, M. Buscaglia, C. Chiccoli, F. Mantegazza, P. Pasini, and C. Zannoni, Phys. Rev. Lett. **85**, 1008 (2000).
[14] T. Bellini, C. Chiccoli, P. Pasini, and C. Zannoni, Mol. Cryst. Liq. Cryst. **290**, 226 (1996).
[15] M. Rotunno, M. Buscaglia, C. Chiccoli, F. Mantegazza, P. Pasini, T. Bellini, and C. Zannoni, Phys. Rev. Lett. **94**, 097802 (2005).
[16] M. Buscaglia, T. Bellini, V. Degiorgio, F. Mantegazza, and F. Simoni, Europhys. Lett. **48**, 634 (1999).
[17] P. A. Lebwohl and G. Lasher, Phys. Rev. A **6**, 426 (1972).
[18] D. J. Cleaver, S. Kraly, T. J. Sluckin, and M. P. Allen, in *Liquid Crystals in Complex Geometries Formed by Polymer and Porous Networks* (Ref. [1]), Chap. 21.
[19] J. Chakrabarti, Phys. Rev. Lett. **81**, 385 (1998).
[20] Y.-K. Yu, P. L. Taylor, and E. M. Terentjev, Phys. Rev. Lett. **81**, 128 (1998).
[21] *Advances in the Computer Simulation of Liquid Crystals*, edited by P. Pasini and C. Zannoni (Kluwer, Dordrecht, 2000).
[22] M. Buscaglia, Ph.D. thesis, University of Pavia, 2000 (unpublished).
[23] A. Glushchenko, H. Kresse, V. Reshetnyak, Y. U. Reznikov, and O. Yaroshchuk, Liq. Cryst. **23**, 241 (1997).
[24] A. Jakli, L. Almasy, S. Borbely, and L. Rosta, Eur. Phys. J. B **10**, 509 (1999).
[25] D. Liang, M. A. Borthwick, and R. L. Leheny, J. Phys.: Condens. Matter **16**, S1989 (2004).